DIM for Detecting Cracks in Masonry Piers with Different Crack Patterns

Ahmed M. Anwar[1]
Adel G. El-Attar[2]
Ahmed M. A. Abd Elwaly[3]

Abstract

In the framework of identifying defects in structures, Damage Index Method (DIM) is considered one of the trustable tools used intensively. In the present research, DIM – modal displacement based - was applied on experimental data to detect damage for masonry piers. Damage Index (D.I.) was obtained by comparing modal displacement functions for damaged and undamaged conditions. Firstly, two scaled down piers were prepared experimentally for examination. The piers were of same unit area while the thicknesses were 170, and 260 mm. The physical models were subjected to different artificial crack patterns. The cracks were created for each pier on three consecutive steps representing different intensity of damage. The piers were examined under free vibration mode at their original state and after degradation. The collected records were processed, and DIM was applied. Furthermore, parametric numerical analysis was used to study the effect of crack dimensions, location, shape, and repetition among the simulated piers. The results showed that the selected D.I. was effective in detecting cracks in masonry structures for all examined cases. Moreover, the investigation showed that as the severity of cracks increased, the identification of damage became easier and was reflected in an increase in D.I. value. DIM was also able to detect expected route of cracks. On the other hand, DIM can't be used to obtain degradation level directly but in comparison between severities of cracks in different stages of damage.

1. Introduction

Performance evaluation of structures is mandatory to keep them healthy during their lifetime span. Damage assessment can be considered useful indicator when applied

[1] Associate Professor, Construction Research Institute, National Water Research Center, Egypt
[2] Professor, Structural Engineering Department, Faculty of Engineering, Cairo University, Egypt.
[3] Assistant Researcher, Construction Research Institute, National Water Research Center, Egypt

periodically. Dynamic testing can be considered as fast non-destructive tool used for this purpose [1]. It can particularly be adopted to identify overall integrity of structures as well as identifying local unseen damages. Continuous and/or periodic monitoring is essential for early damage detection. Generally, full damage identification procedure can follow four stages (detection, localization, quantification, and prediction). Global vibration-based damage detection methods such as capturing the changes in natural frequency could be limited to detect degradation in structural integrity. Modal strain energy approach could add better information about crack locations. Advanced damage detection techniques (e.g., Wavelet analysis, artificial neural network, and acoustic emission monitoring) could be more trustable in identification and quantification of damage in structures.

The challenge becomes higher when dealing with structures of sophisticated special nature such as masonry piers where bonding between mortar and bricks build-up the final structure. Deterioration in such structures can be expressed by aging, interfacial debonding between mortar and brick units, and damage in either bricks or mortar independently [2-5]. Many researchers used several damage indicator tools based on dynamic measurements [6-9]. Stubbs et al. [10] suggested the damage index method to detect the damage in real existing bridge using comparison in strain energy in separate structural elements. Cornwell et al. [11] compared principal curvatures of plates in different degradation conditions. Maghsoodi et al. [12] applied Euler-Bernoulli concept for detecting damages in beams. Qiao et al. [13] investigated mode shape curvature method as a technique of damage detection to identify damage in composite laminated plates. Other researchers [14–16] have made modifications to Damage Index Method (DIM) for damage detection and health monitoring of structures.

In the current research, formal DIM was used to determine the location of cracks in masonry piers. Contrast between normalized modal displacements in damaged and virgin conditions was taken as Damage Index (D.I.). DIM was applied experimentally to accommodate the special behavior of masonry structures. Moreover, the effect of limited monitoring points on identifying cracks was also studied. Two masonry piers of different thicknesses and different crack configurations were represented experimentally. Modal analysis was performed for damaged and undamaged specimens. Simultaneously, numerical parametric investigation was also conducted to determine the effect of damage severity, crack shape, location as well as the existence of multiple cracks on the identification process. The method showed good results in identifying cracks in masonry piers.

2. Methods and Methods

In the current paper, DIM was used as a tool for determining local damages occurred in masonry piers. D.I. based on comparing damaged and undamaged normalized modal displacement functions obtained directly from modal analysis of structures was adopted. In fact, many researchers stated that depending on modal displacement vectors were of lesser sensitivity to detect small damages rather than using modal strain energy functions [17, 18]. It is however, in case of few or irregular distribution of monitoring points - where obtaining curvature functions are of quite difficult operations - the adequacy of using D.I., modal displacement based, should be checked. The modal normalized displacement shape function will be denoted as (Φ) and will be obtained hereinafter using formal modal analysis from the measured vibration. The value of normalized modal displacement at the edge of a given element at jth node of the pier in damaged and undamaged states can be represented by ($\Phi_{j, D}$) and ($\Phi_{j, U}$), respectively. The fractional energy exerted by this element in damaged and

undamaged condition can be expressed as (Fj, D) and (Fj, U), respectively. n denotes for the total number of nodes.

$$F_{j,D} = \frac{\Phi_{j,D}}{\sum_1^n \Phi_{n,D}} \tag{1}$$

$$F_{j,U} = \frac{\Phi_{j,U}}{\sum_1^n \Phi_{n,U}} \tag{2}$$

Where, total energy exerted by the structure can be denoted by E_D and E_U for damaged and undamaged conditions, respectively, and can be represented as follow.

$$E_D = \sum_1^n \Phi_{n,D} \qquad \text{and} \qquad E_U = \sum_1^n \Phi_{n,U} \tag{3,4}$$

It should be noted that summation of fractional energy over the whole system should be equal to unity. Thus,

$$\sum_1^n F_{j,D} = \sum_1^n \frac{\Phi_{j,D}}{E_D} = 1 \qquad \text{and} \qquad \sum_1^n F_{j,U} = \sum_1^n \frac{\Phi_{j,U}}{E_U} = 1 \tag{5,6}$$

If the damage is particularly assumed to be located at a single element, then the fractional energy remains relatively constant, i.e. $F_{i,D} \approx F_{i,U}$. Assuming the term Φ_D and Φ_U denotes for vectors containing $F_{i,D}$,and $F_{i,U}$ respectively, for n nodes. Thus,

$$\Phi_D = \left\{ F_{j,D} \Big|_{j=1}^{n} \right\}_{n\,x1} \qquad \text{and} \qquad \Phi_U = \left\{ F_{j,U} \Big|_{j=1}^{n} \right\}_{n\,x1} \tag{7,8}$$

Simply, one can define D.I. as a vector of size (n x 1) where all its values should equal unity in case of no damage, where the values could have values greater than unity in case of damage exists.

$$D.I. = \frac{\Phi_D}{\Phi_U} \tag{9}$$

Plotting the D.I. values among the pier surface using suitable grid allowed having a peak value around the location of damages.

3. Experimental Work

Two masonry piers made from clayey bricks and mortar were constructed and examined. Mechanical properties of bricks and mortar were test experimentally and was found in agreement with Narayanan S. P. and Sirajuddin M. [19]. Table (1) shows the physical and mechanical properties of masonry piers' constitutional material. The piers were of typical elevational dimensions (width x height) equal to (1m x 1m). The First pier was of thickness

170 mm, and totally made of clayey red bricks and having the prefix of (P170). The second pier was of total thickness 260 mm and composed of double wythe masonry encasing each of thickness 85 mm incorporated mortar core of thickness 90 mm and was denoted as (P260). The later pier was intentionally constructed to simulate real piers used in old hydraulic structures. All piers were clamped to the floor using steel frames fixed to the ground by means of suitable anchor bolts, Figures (1a – c) show piers in their original state along with the base frame. In this way, all base translations in all orthogonal directions were restrained, simultaneously, semi-rigid rotational restraint among the minor axis of the piers was assumed. Each pier was equipped with available seven accelerometers. Figures (2a and b) show accelerometers arrangement, and schematic illustrating the used crack patterns. Figure (3) shows typical cross-sectional area for both tested piers.

Artificial horizontal cracks at level 170 mm from ground were created for both piers. The cracks were executed using mechanical saw cut of blade thickness of 4 mm. The severity of cracks was increased in three consecutive steps. For each step, the originally generated crack got further deeper and longer. The first crack was of 400 mm length and 20 mm depth. The cracks were then enlarged in steps with incremental increase of 200 mm in length and 20 mm in depth. Table (2) describes and gives detailed configuration for examined piers. Generally, all piers were examined in free vibration fashion. The piers were excited using small mass impact hummer striking the piers horizontally at the midpoint of their top level. The forced vibration time-history was omitted, and the rest of the record was analyzed. The piers were examined at different stages; the first stage represented initial records of the piers in their original healthy state. The following stages were for damaged piers at different severities. To capture all available modes with reasonable accuracy, sampling rate of 1KHz was adopted. The records were analyzed, mode shapes were obtained, and Fast Fourier Transformation (FFT) were conducted. Figures (4 and 5) show monitored time history records and FFT plots for examined specimens at undamaged condition for accelerometer at (CH2). Table (3) shows dominant frequencies and corresponding mode shapes for examined specimens. The proposed DIM was then applied on the tested piers and crack locations were estimated.
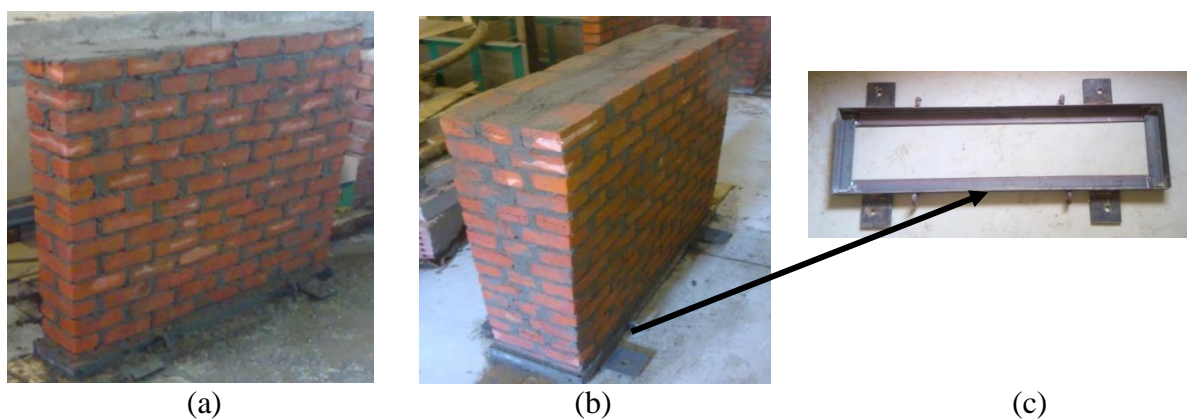

(a) (b) (c)

Figure 1: Physcial model for Masonry Piers in Original Condition a) P170, b) P260, and c) Supporting Steel Base
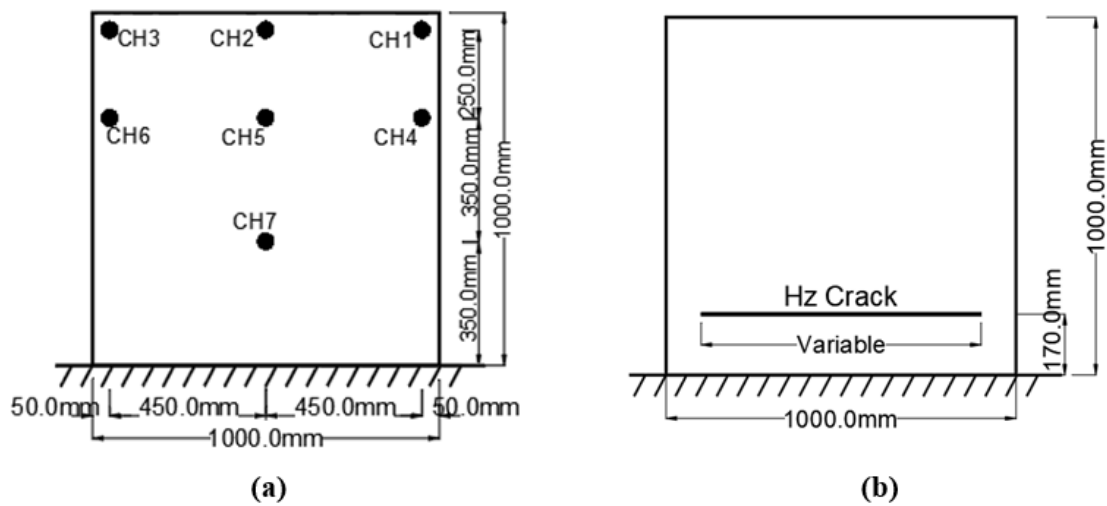
Figure 2: a) Schematic Showing Accelerometers Arrangement, and b) Horizontal Crack Pattern for Examined Specimens
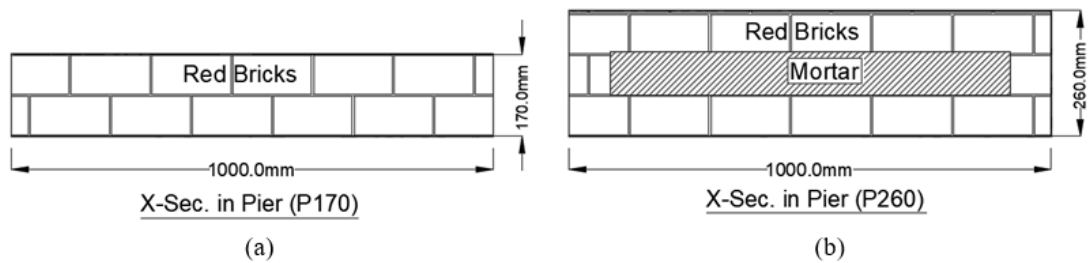

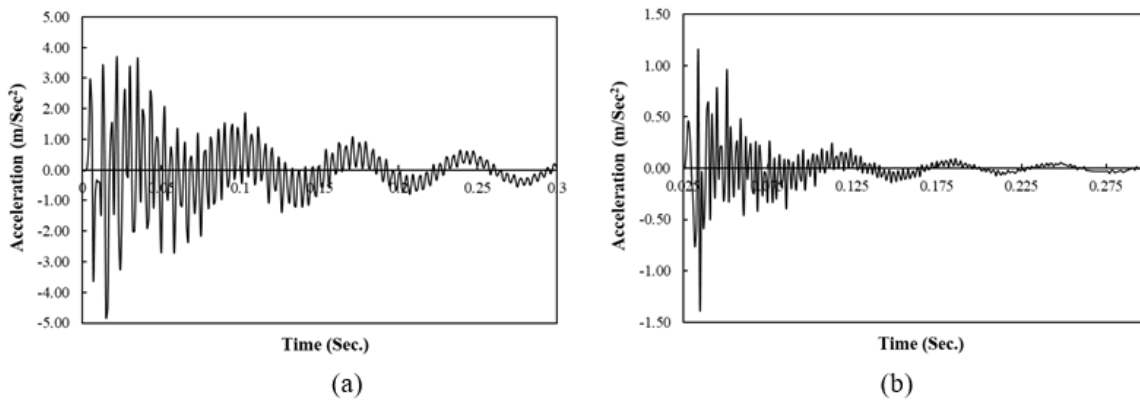Figure 3: Cross Sectional Area of Examined Piers a) P170, and b) P260

Figure 4: Acceleration Time History for a) P170, and b) P260 in Undamaged Condition
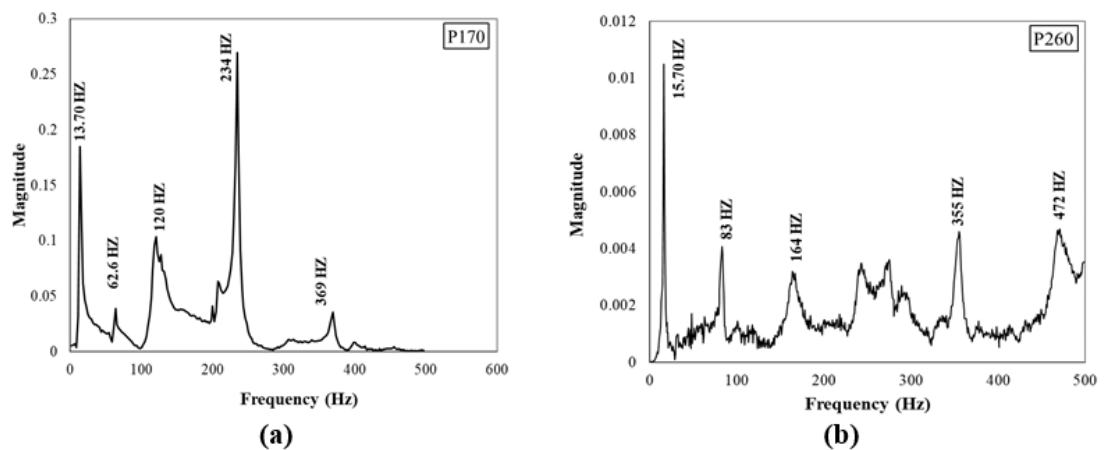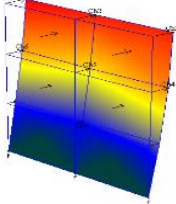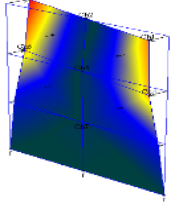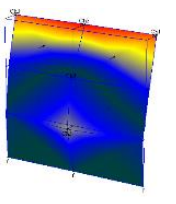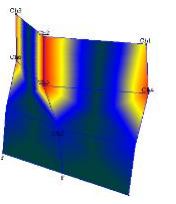

Figure 5: FFT for a) P170, and b) P260 in Undamaged Condition

Table 2: Description of Examined Piers

Pier	Specimen	Horizontal Crack Dimensions	
		Length (mm)	Depth (mm)
P170	(P170-H-C-400-20)	400	20
	(P170-H-C-600-40)	600	40
	(P170-H-C-800-80)	800	80
P260	(P260-H-C-400-20)	400	20
	(P260-H-C-600-40)	600	40
	(P260-H-C-800-80)	800	80

Table 3: Dominant Frequencies and Corresponding Mode Shapes for Examined Piers

Virgin Sample	Dominant Mode Shapes - (Hz)			
	First Bending	First Torsion	Second Bending	Combined Mode
P170	13.70	62.60	120.00	234.00
P260	15.70	82.60	1640.00	355.00

4. Results and Discussion

Formal modal analysis was conducted on damaged piers and their dynamic properties were obtained using (ME' Scope) [20]. The obtained parameters were then compared with their corresponding values of virgin specimens. Fast Fourier Transformation (FFT) of all damage cases with horizontal cracks were plotted. Natural frequencies of the dominant mode shape were shown at each corresponding peak. Comparison with the control specimens was conducted. It was noted that significant decrease in all natural frequencies with the increase in crack length and depth was observed. DIM was applied where normalized modal displacements (Φ) were used to calculate D.I. Modal displacement was normalized with respect to maximum displacement value at the top level of piers. D.I. having values greater than unity indicated possibilities of damage existence. At each joint of the pier, D.I. was plotted over the whole pier. The created surface with humps indicating presence of cracks. The Plots were created using Sigma Plot V.11.0 [21]. The program allows, only, to draw the independent variables in the vertical direction. Thus, the coordinates of the pier were compulsory plotted in plan and D.I. values were drawn parallel to vertical axis. Figures (6a – c) show FFT plots for all damage cases of specimens P170. Figures (7a – c) represents the location of probable cracks under the horizontal projection of the created surface at the peak value of D.I. for all damage scenarios of P170. Similarly, Figures (8a – c) show FFT plots for all damage scenarios for P260. Figures (9a – c) explain the location of cracks for all degradation conditions of P260.

It was observed that the natural frequency of the first bending mode shape of the undamaged case for (P170) was 13.70 Hz. The natural frequencies of damaged cases became 13.20 Hz for (P170-H-C-400-20) and reached to 10.80 Hz for (P170-H-C-800-80). On the other hand, it was noticed that the D.I. values increased with increasing the damage length and depth. The D.I. started with 1.18 for (P170-H-C-400-20) and reached to 1.6 for

(P170-H-C-800-80). On the other hand, the natural frequency of the first bending mode for (P260) was 15.70 Hz while the natural frequencies of damaged cases decreased to 15.20 Hz for (P260-H-C-200-20) and reached 14.40 Hz for (P260-H-C-800-80). D.I. value started with 1.16 for case (P260-H-C-200-20) and reached to 1.25 for case (P260-H-C-800-80). The peak in the plot of DI indicated the crack location. Despite using modal displacement as damage indicator with relatively small number of sensors, DIM proved its efficiency to detect and locate the crack location using only seven sensors. It was clear that these peaks increased by increasing cracks' dimensions, length, and depth. It can be observed that as cracks got severer, the damage detection procedure became easier. On the other hand, it was clear that for the same crack dimensions, the pier with lesser stiffness had D.I. values greater than the stiffer pier. In fact, the existing of stiff mortar core has big effect on preserving the rigidity of the pier and minimize the crack effect. Thus, slightly decreasing D.I. values for composite pier (P260).
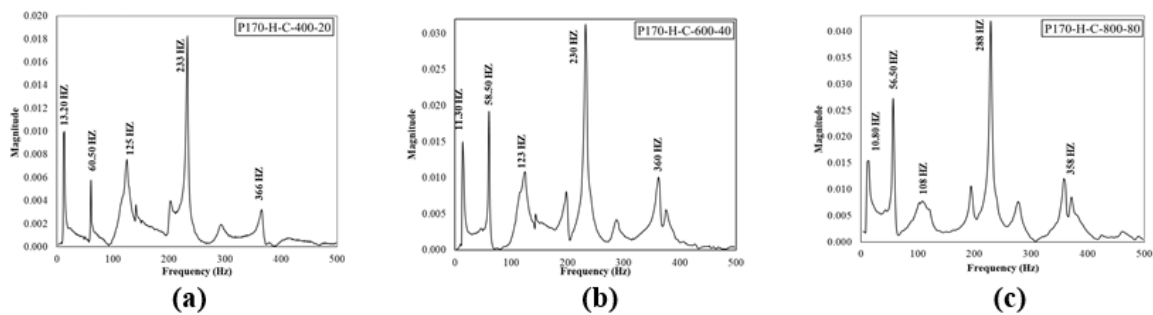

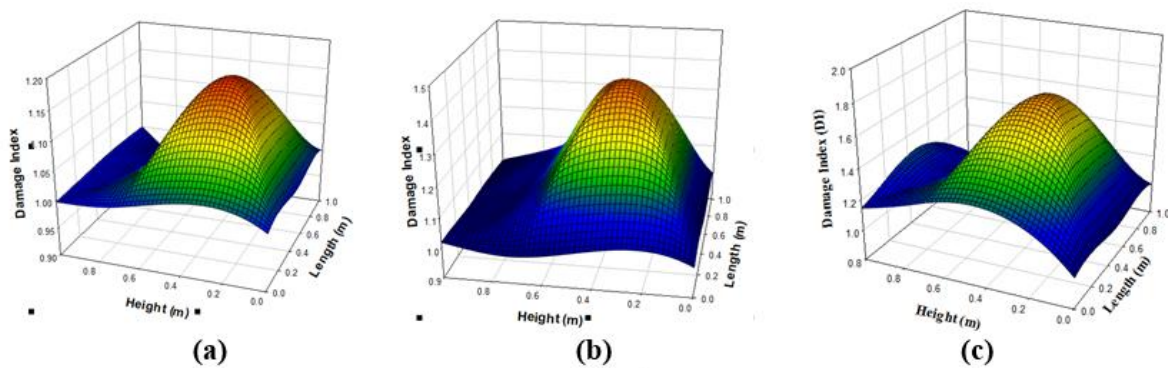Figure 6: FFT for All Damaged Scenarios of P170

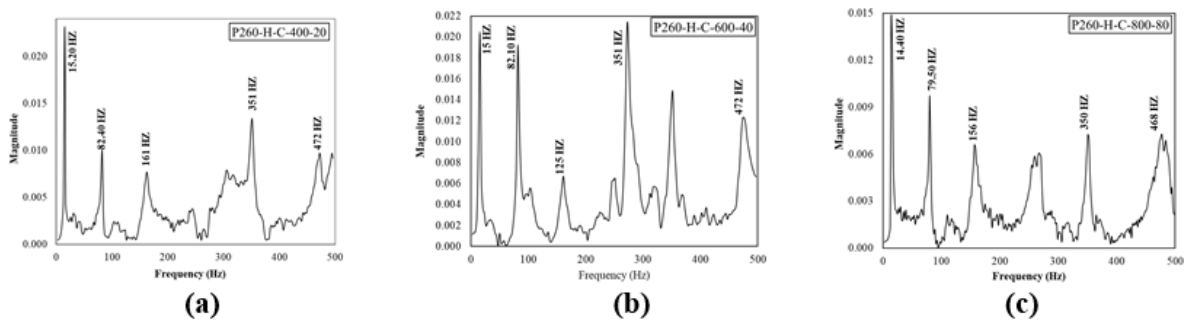Figure 7: D.I. Plots for All Damaged Scenarios of P170
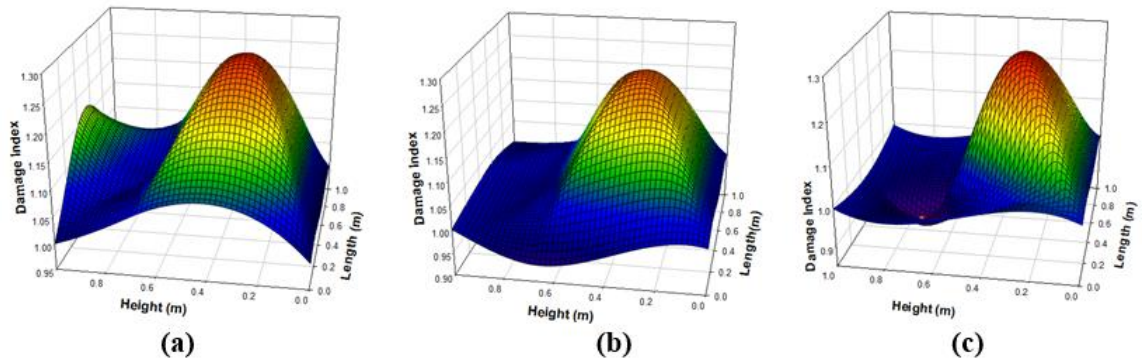

Figure 8: FFT for All Damaged Senarios of P260

Figure 9: D.I. Plots for All Damaged Senarios of P260

5. Parametric Study

5.1. Numerical Model Calibration

In this section, numerical analysis was conducted to study the effect of crack severity in the identification process. In fact, masonry structures are composed of heterogeneous materials composed of blocks and mortar joints. Detailed analysis should be done in micro-modeling scale to represent units, mortar, and unit/mortar interface. This can be helpful for small structural elements with particular interest in the heterogeneous states of stress and strain among their constituents and the interface. Moreover, complicated models are required when dealing with large deformation problems or studying mechanical behavior of masonry till failure [21]. On the other hand, Laurance [22] stated that macro-scale models can be good representative for simulating large scale systems where knowledge about interaction between units and mortar can be negligible for the sake of global structural behavior. He also added that in simplified modelling, brick and mortar were modeled as a single smeared material and the mortar joints were modeled as zero-thickness interfaces. Alternatively, composite behavior in terms of macro or average stresses and strains can be used to model masonry as a homogeneous material [23]. In this case, extensive experimental data should be used for validation. On the other hand, SAP2000 [24] was also used by recent researchers where non-linear shell elements were adopted to simulate unreinforced masonry buildings subjected to ground motions [25].

In the current research, constitutive linear modeling was used to represent masonry piers. Homogeneous isotropic behavior of masonry was simulated using shell elements. This can be good assumption only for case of small deformations with relatively small level of stresses. Many trials were conducted to adjust the Finite Element (FE) model with the experimental work. The boundary conditions of the model were firmly restrained at the base in vertical and horizontal directions. Rotational springs were also used, and their stiffness were adjusted until matching with the experimental modal analysis. The calibration was accepted when the dominant natural frequencies almost coincided with those obtained experimentally. On the other hand, Cracks were simulated as a reduction in shell thickness. In this situation the pier was considered as continuum system with variable inertia. It is worth to mention that the results of the numerical work could be limited to the conditions under which the data were obtained.

Piers (P170), and (P260) were firstly simulated in their undamaged conditions using shell elements. Figure (10) shows uncracked FE model for (P170). The first dominant frequencies of (P170) and (P260) was 14.10, and 15.92 Hz, respectively. The corresponding values obtained experimentally were 13.70, and 15.70 Hz, with acceptable error of 2.9%,

and 1.38%, respectively. This indicates that the FE modeling was acceptable to be used for parametric study.
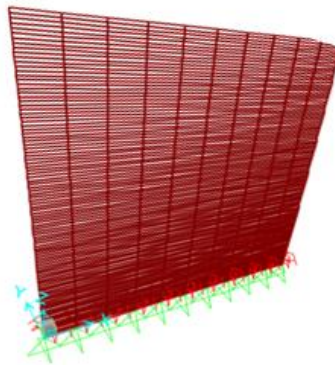

Figure 10: Finite Element Uncracked Model for P170

5.2. Horizontal Cracks

Write DIM was applied on Finite Element (FE) pier models with dimensions typically like those used in the experimental work. Horizontal cracks were all located at distance 170 mm from the base. Variation in damage intensity was executed by changing crack length and depth. Crack depth was chosen as a percentage of pier thickness, 25%, 50%, and 75%, of pier thickness. Variation of crack length started from 0.2L (200 mm) to 1L (1000 mm) with incremental increase of 0.2L.

Table 4: Natural Frequencies for (P170) and (P260) with Different Damage Scenarios
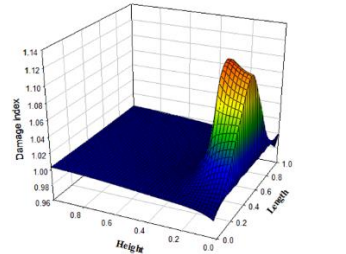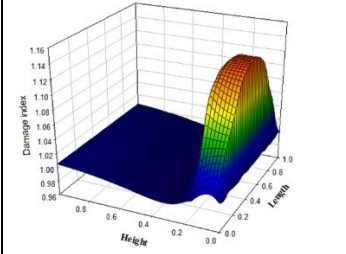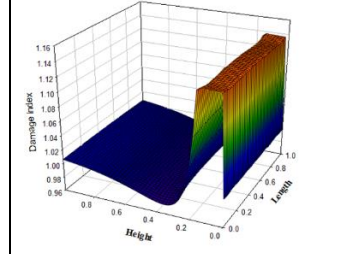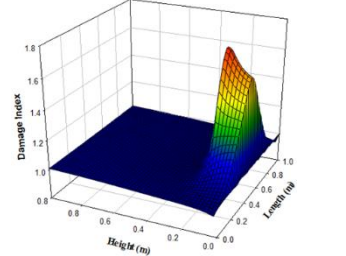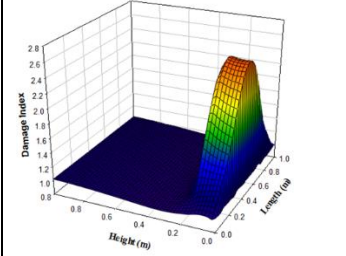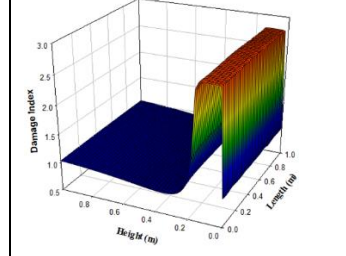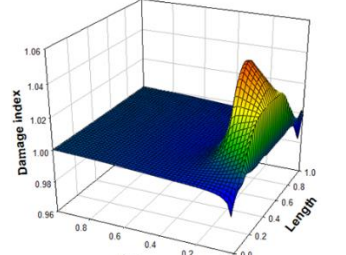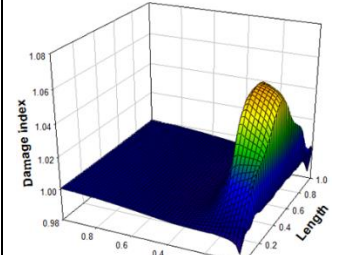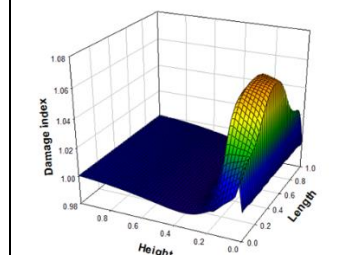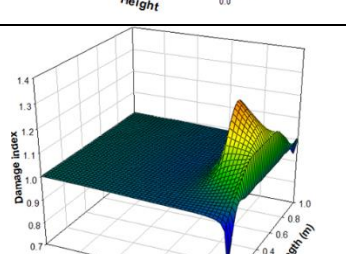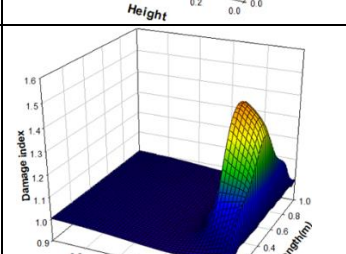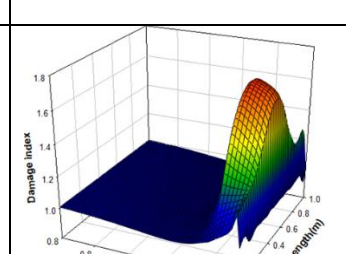
Pier	Crack Depth (%) of Pier Thickness	Frequency (Hz) – (Stiffness Reduction) (%)				
		Damage Length				
		0.2L	0.4L	0.6L	0.8L	1L
P170	25	14.09 - (0.14)	14.07 - (0.43)	14.06 - (0.57)	14.04 - (0.85)	14.02 - (1.13)
	50	14.06 - (0.57)	14.00 - (1.41)	13.94 - (2.26)	13.87 - (3.24)	13.76 - (4.76)
	75	14.01 - (1.27)	13.80 - (4.21)	13.47 - (8.74)	13.04 - (14.47)	11.68 - (31.38)
P260	25	15.89 - (0.38)	15.89 - (0.44)	15.88 - (0.50)	15.87 - (0.63)	15.86 - (0.75)
	50	15.87 - (0.63)	15.84 - (1.00)	15.81 - (1.38)	15.78 - (1.75)	15.70 - (2.74)
	75	15.84 - (1.00)	15.74 - (2.25)	15.58 - (4.23)	15.37 - (6.79)	14.65 - (15.32)

Table (4) represents the dominant frequencies for all damaged cases for both tested piers. The Table also shows the percentage of stiffness reduction for each condition. The modal displacement shape functions of the first mode were extracted for all damage cases and used to compute the D.I. Numerically, records from each node of the FE model were processed. Table (5) explains the effect of crack severity on the identification process. Damages of depths 50%, and 75%, and lengths of 0.4L, 0.8L, and 1L were selected and only expressed in this Table. The selected conditions represented critical cases that can be considered as

moderate or severe damages. Damage Index plots were compared, and it was noticed that the peak of the created surface represented the location of damage. The D.I. value increased with increase in the damage severity.

Further, summary of all results is represented in Figures (11a, and b) for (P170) and (P260), respectively. The plots explain that D.I. values were directly proportional with severity of cracks. It was shown that the peaks values and sizes of D.I. increased with the increase of the thickness and the size of the damage with an agreement to experimental results. It can also be noted that for (P170), D.I. values were higher than those of (P260). This could be attributed to the higher degradation happened in (P170) compared to (P260) when exposed to same crack. It was noted that for (P170), DI peak values were ranged from 1.01 to 1.08 in case of 25% cracked depth and increased to the range of 1.3 to 2.8 in case of 75% cracked depth. The corresponding values for (P260) were of range of 1.005 to 1.03 in case of 25% cracked depth and 1.1 to 1.6 in case of 75% crack depth. Finally, it was concluded that DIM, modal displacement based, proved its efficiency to detect and locate the crack location experimentally and numerically.

Table 5: D.I. Values Obtained Numerically for Examined Piers

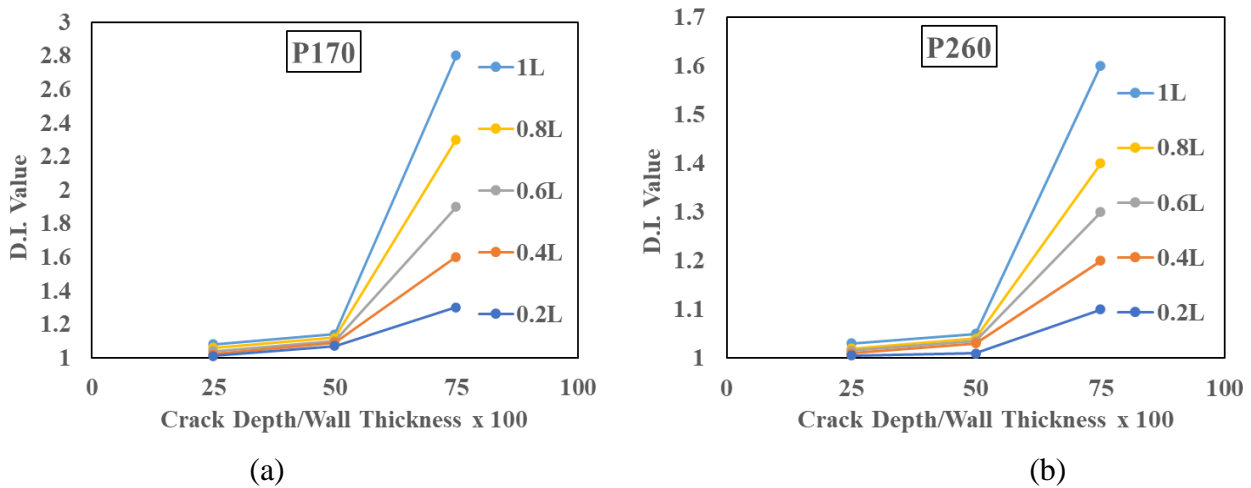| Pier	Damage Depth %	Damage Length		
		0.4L	**0.8L**	**1L**
P170	50%			
	75%			
P260	50%			
	75%			

Figure 11: Peak D.I. Values for a) P170, and b) P260

5.3 Multiple and Inclined Cracks

In this section DIM technique was examined to detect different shapes of defects that possibly be created on reality among masonry piers. For simplicity, Pier (P170) was selected for examination only. Single and double vertical cracks, inclined crack, and stepped crack were tried. Crack was typically simulated as a reduction in the pier thickness at crack location (50% of pier thickness). Single vertical crack was examined; the crack was 400 mm length, started at 200 mm from the base and located at 300 mm from the right side of the pier. Further, double vertical identical cracks of length of 600 mm started at 200 mm from the base of the pier and located at 300 mm far from each of the sides of specimen. As per inclined crack, the crack was created at 45 degree, its horizontal and vertical projections were 400 mm and the crack started at 400 mm from the left side and ended at 200 mm from the right side. Finally, stepped zigzag shape following the mortar pass of three successive brick units was also tried. Formal modal analysis was conducted and the same procedure for obtaining D.I. was followed. The analysis was done based on the dominant first mode. Figures (12 – 15) show schematics for the crack shape and the corresponding DI plot for all cases. It was observed that modal displacement also was trustable index and was sufficient to locate cracks regardless their shape and repeatedly.
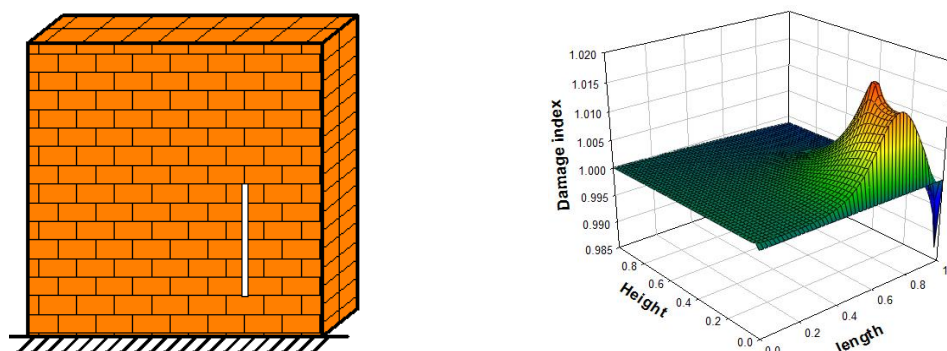

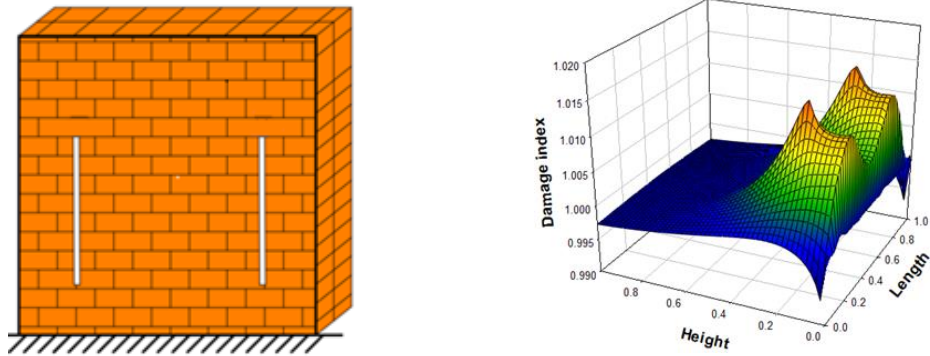Figure 12: D.I. of Single Vertical Crack

Figure 13: D.I. of Double Vertical Cracks
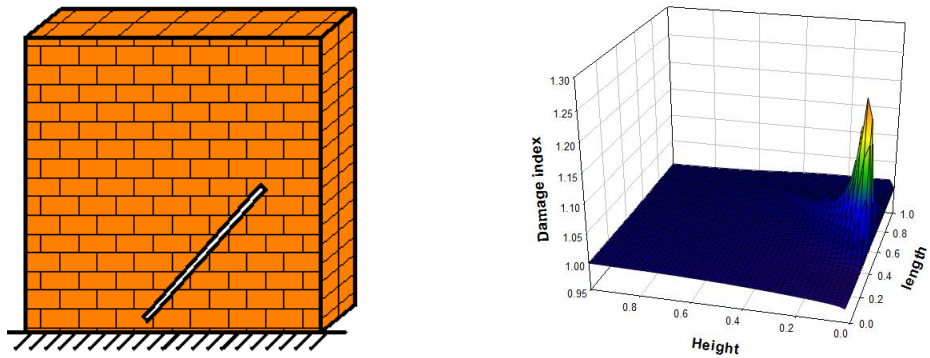
Figure 14: D.I. of Inclined Crack
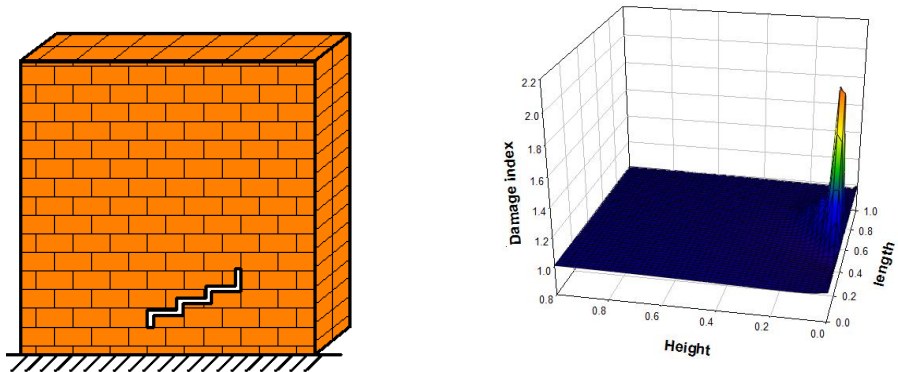
Figure 15: D.I. of Zigzag Stepped Crack

6. Conclusions

Damage detection in masonry structures based on DIM, modal displacement based, was conducted. Physical and numerical modeling were used to verify the adequacy of using the proposed method. The following conclusions were obtained:

1- D.I. has good ability to identify single horizontal cracks for both experimental and numerical models.

2- Experimentally, the results showed that modal displacement functions could be sufficient to detect defects in sophisticated nature of masonry piers even when only limited recorded data were available.

3- It was also observed that DIM could be used for comparing between severities of cracks in similar structures and found to be directly proportional with D.I. value.

4- For the same crack dimensions, the stiffer the pier rigidity, the more difficult the identification of damage.

5- It was noted that for masonry structures, non-linear simulation can be possible for low level of stresses and small deformations.

6- Numerically, vertical, inclined, stepped, and multiple cracks were identified using the proposed technique.

7- The present results constitute the first step of a work in progress. Further intensive numerical non-linear simulation of masonry as an orthotropic material with particular care to interface modeling should be adopted.

References

[1]   D. Foti, "Dynamic Identification Techniques to Numerically Detect the Structural Damage," Open Constr. Build. Technol. J., vol. 7, no. 1, pp. 43–50, 2013.

[2]   S. Dimovska and N. Serdar, "The Mechanical Properties of Masonry Walls- Analysis of the Test Results, " proceeding of International Scientific Conference Urban Civil Engineering and Municipal Facilities, vol. 117, pp. 865–873, 2015.

[3]   M. Bošnjak-klečina and S. Lozančić, "Testing of Physical and Mechanical Properties of Bricks and Mortar in Historic Structures," Technical Gazette 17, pp. 209–215, 2010.

[4]   Y. Wu, S. Li, D. Wang, "Characteristics of acoustic emission signals of masonry specimens under uniaxial compression test", Construction and Building Materials, 196, pp. 637 – 648, 2019. https://doi.org/10.1016/j.conbuildmat.2018.11.148

[5]   A. M. A. Abd Elwaly, "Damage Detection in Masonry Piers of Hydraulic Structures using Dynamic Measurements", M. Sc. Thesis, Faculty of Engineering, Cairo University, 2020.

[6]   S.H. Sung, H.J. Jung, H.Y. Jung, "Damage detection for beam-like structures using the normalized curvature of a uniform load surface", J. Sound and Vibration, V 332, Issue 6, pp. 1501 – 1519, 2013. https://doi.org/10.1016/j.jsv.2012.11.016

[7]   C. Michel, A. Karbassi, P. Lestuzzi, Evaluation of the seismic retrofitting of an unreinforced masonry building using numerical modeling and ambient vibration measurements, Eng. Struct. 158, 124–135, 2018.

[8]   S.M.H. Pooya and A. Massumi, "A novel and efficient method for damage detection in beam -like structures solely based on damaged structure data and using mode shape curvature estimation", J. Applied Mathematical Modelling, 91, 670-694, 2021. https://doi.org/10.1016/j.apm.2020.09.012

[9]   F. Sadeghi, Y. Yu, X. Zhu, J. Li, "Damage identification of steel-concrete composite beams based on modal strain energy changes through general regression neural network", J. Engineering Structures, 244, 112824, 2021. https://doi.org/10.1016/j.engstruct.2021.112824

[10] N. Stubbs, J. T Kim and C. R Farrar, "Field verification of a nondestructive damage localization and severity estimation algorithm," Proc. 13th Int. Modal Anal. Conf. (IMAC XIII), vol. 182, no. August 2016, pp. 210–218, 1995.

[11] P. Cornwell, S. W. Doebling, and C. R. Farrar, "Aplication of the strain energy damage detection method to plate-like structures ," Journal of Sound and Vibration, Vol. 224, pp. 359–374,1999.

[12] A. Maghsoodi, A. Ghadami, and H. R. Mirdamadi, "Multiple-crack damage detection in multi-step beams by a novel local flexibility-based damage index," J. Sound Vib., vol. 332, no. 2, pp. 294–305, 2013.

[13] P. Qiao, K. Lu, W. Lestari, and J. Wang, "Curvature mode shape-based damage detection in composite laminated plates," J. compsite structures, vol. 80, pp. 409–428, 2007.

[14] F. C. Choi, J. Li, B. Samali, and K. Crews, "Application of the modified damage index method to timber beams," Eng. Struct., vol. 30, No. 4, pp. 1124–1145, 2008. http://dx.doi.org/10.1016/j.engstruct.2007.07.014

[15] A. Maghsoodi, A. Ghadami, and H. R. Mirdamadi, "Multiple-crack damage detection in multi-step beams by a novel local flexibility-based damage index," J. Sound Vib., vol. 332, No. 2, pp. 294–305, 2013. https://doi.org/10.1016/j.jsv.2012.09.002

[16]   T. You, P. Gardoni, and S. Hurlebaus, "Iterative damage index method for structural health monitoring", Structural Monitoring   and Maintenance, Vol. 1, No. 1, pp. 89–110, 2014. http://dx.doi.org/10.12989/smm.2014.1.1.089

[17]   L.H. Yam, T.P. Leung, D.B. Li, and K.Z. Xue, "Theoretical and experimental study of modal strain analysis", J. of Sound and Vibration, 191 (2), pp. 251-260, 1996.

[18]   F. Wang, R. Li, Y. Xiao, Q. Deng, X. Li, and X. Song, "A strain modal flexibility method to multiple slight damage localization combined with a data fusion technique", Measurement, 182, 109647, 2021,. https://doi.org/10.1016/j.measurement.2021.109647

[19]   S. P. Narayanan and M. Sirajuddin, "Properties of Brick Masonry for FE modeling," Am. J. Eng. Res., no. 1, pp. 2320–847, 2013.

[20]   ME'Scope, 2005, User Manual, Vibrant technology, U.S.A.

[21]   SigmaPlot, V. 11.0, Copyright © 2008, Systat Software, Inc., Germany.

[22]   A. Rafiee, M. Vinches, "Mechanical behavior of a stone masonry bridge assessed using an implicit discrete element method", Engineering Structures, 48, pp. 739-749, 2013. http://dx.doi.org/10.1016/j.engstruct.2012.11.035

[23]   Paulo B. Lourenco, "Computational Strategies for Masonry Structures", Delft University Press, Stevinweg 1, 2628 CN Delft, The Netherlands, 1996. https://www.researchgate.net/publication/27344834

[24]   Pieruszczak, S., Niu, X., "Mathematical description of macroscopic behavior of brick masonry", Int. J. Solids Structures, 29 (5), pp. 531 – 546, 1992.

[25]   SAP2000, 2009. CSI: Computers and Structures Inc, Version 14.1.0. Computer software.

[26]   Daniele Losanno, Nagavinothini Ravichandran, Fulvio Parisi, Andrea Calabrese, Giorgio Serino, "Seismic Performance of a Low-cost isolation system for unreinforced brick Masonry buildings in developing countries", Soil Dynamics and Earthquake Engineering, 141, 106501, 2021. https://doi.org/10.1016/j.soildyn.2020.106501

استخدام طريقة معامل الضرر للكشف عن الأعطاب للبغال المبنية من الطوب

الملخص

يمكن تعريف الضرر بوجود أي تغير في خصائص المنشأ أو أبعاده الهندسية نتيجة لتأثره بالعوامل الجوية أو ظهور الشروخ عليه. ويعتبر تحديد الأضرار في مراحل متقدمة أمر ضرروي للحفاظ على سلامة المنشأ وخصوصاً في المنشآت ذات الطبيعة الخاصة مثل بغال الطوب والمستخدمة في العديد من منشآت الري القديمة مثل الكباري والقناطر. وقد تم في هذا البحث استخدام الاختبارات ديناميكية غير المتلفة لتحديد أماكن الشروخ في البغال من الطوب الأحمر الطيني والتي تتميز بالسرعة والسهولة مقارنة ببعض الطرق المتلفة الأخري. وقد تم استخدام طريقة "معامل الضرر" للكشف عن الأعطاب بأشكالها المختلفة والمتوقعة للمباني من الطوب والتي تعتمد بشكل كبير على عمل مقارنة للأشكال النمطية الطبيعية للمنشآت في الحالة السليمة وكذلك الحالة التي تحتوي على شروخ. وقد تم الاستعانة بالنماذج المعملية لحائطين من الطوب والمونة بأسماك مختلفة حيث تم اختبارهما تحت تأثير الاهتزاز الحر وعمل التحليلات الطيفية واستنتاج الخصائص الديناميكية لهما. كما تم عمل نماذج رياضة مساعدة لتمثيل أشكال متعددة من الشروخ بالحوائط تحاكي الطبيعة حيث تم تطبيق طريقة "معامل الضرر" لتحديد أماكن الشروخ. وقد خلصت الدراسة بقدرة الطريقة المستخدمة على تحديد أماكن الشروخ لكلٍ من النماذج الطبيعية والعددية بشكل مرضي وامكانية استخدام تلك الطريقة للمقارنة بين شدة الشروخ وحجم الضرر للحالات المختلفة.

الكلمات الدالة:　　الشروخ، معامل الضرر، البغال من الطوب، القياسات الديناميكية.